

## Electronic Supporting Information

# **Multi-resonance organoboron-based fluorescent probe for ultra-sensitive, selective and reversible detection of fluoride ion**

Yanyu Qi,<sup>a,b</sup> Xiaosong Cao,<sup>a</sup> Yang Zou\*<sup>a</sup> and Chuluo Yang\*<sup>a,c</sup>

<sup>a</sup> Shenzhen Key Laboratory of Polymer Science and Technology, College of Materials Science and Engineering, Shenzhen University, Shenzhen 518060, People's Republic of China

<sup>b</sup> College of Physics and Optoelectronic Engineering, Shenzhen University, Shenzhen 518060, People's Republic of China

<sup>c</sup> Hubei Key Lab on Organic and Polymeric Optoelectronic Materials, Department of Chemistry, Wuhan University, Wuhan, 430072, People's Republic of China.

### **Corresponding authors**

\*Email: yangzou@szu.edu.cn

\*Email: clyang@szu.edu.cn

Experimental Section.....	2
Figures and Schemes.....	5

## Experimental Section

**Materials.** All reagents and chemicals (at least analytical grade) were purchased from commercial sources and immediately used without further purification. Solvents were all dried and degassed using the Grubbs-type solvent purification system, a product of Innovative Technology, Inc. Schlenk technology was strictly performed under argon conditions in all reactions. The target compound **BNCz** was synthesized and characterized according to the literature.<sup>1</sup>

**Instrumental Methods.** <sup>1</sup>H NMR and <sup>13</sup>C NMR spectra were acquired on Bruker AV 600 NMR spectrometer at room temperature using CDCl<sub>3</sub> as solvent, and referenced externally to SiMe<sub>4</sub>. The multiplicities of the signals are indicated as “s”, “d”, “t” or “m”, which stand for singlet, doublet, triplet, and multiplet, respectively. Carbon atoms directly bonded to boron atom are not always observed in the <sup>13</sup>C NMR spectra due to quadrupolar relaxation leading to considerable signal broadening.<sup>2-4</sup> <sup>11</sup>B NMR spectra were recorded on Bruker AV 600 NMR spectrometer at room temperature using CDCl<sub>3</sub> and tetrahydrofuran-d<sub>8</sub> as solvent, and chemical shifts (δ) are given in ppm relative to BF<sub>3</sub>·OEt<sub>2</sub>. High-resolution mass spectra (HRMS) were collected on a Bruker maxis UHR-TOF mass spectrometer in an ESI positive mode. UV-Vis spectra in solution were recorded on a UV-3100 spectrophotometer at room temperature. Steady-state fluorescence emission spectra were performed at room temperature on a Hitachi F-7000 fluorescence spectrophotometer with xenon lamp as the light source. The absolute fluorescence quantum yields were measured on a Quantaaurus - QY measurement system (C9920-02, Hamamatsu Photonics) equipped with a calibrated integrating sphere and were excited at 467 nm. During the PLQY measurements, the integrating sphere was purged with pure and dry argon to maintain an inert environment. The fluorescence lifetime measurements were performed at room temperature on a single photon counting spectrometer from Edinburgh Instruments (FLS920) with a Picosecond Pulsed UV-LASTER (LASTER377) as the excitation source. The optical images were recorded using a Canon 70D camera.

**X-ray Crystallography.** Crystals of appropriate quality for X-ray diffraction studies were removed and covered with a thin layer of hydrocarbon oil (Paratone-N). A suitable crystal was then selected, attached to a glass fiber. All data were collected using a Bruker APEX II CCD detector/D8 diffractometer using Ga/Cu K $\alpha$  radiation. The data were corrected for absorption through Gaussian integration from indexing of the crystal faces. Structures were solved using the direct methods

programs SHELXS-97, and refinements were completed using the program SHELXL-97.<sup>5</sup> The crystallographic information has been deposited with Cambridge Crystallographic Data Centre, and signed to CCDC code 2032277 for **BNCz**, and 2032276 for **BNCz-FO**.

**Theoretical Calculations.** The ground state geometries of gas state were fully optimized by B3LYP method including Grimme's dispersion correction with 6-31G (d, p) basis sets using Gaussian 09 software package<sup>6</sup>. HOMO and LUMO were visualized with Gaussview 5.0.

**Photochemical Stability.** The photochemical stability of **BNCz** in THF solution was tested using a Hitachi F-7000 fluorescence spectrophotometer with a time scan pattern and a 150 W Xenon lamp was employed as the light source. Typical irradiation time was 2.5 h.

**Anion sensing studies.** Stock solutions (1 mM) of probe **BNCz** was prepared in THF and the final concentrations were 10  $\mu\text{M}$  by a 100x dilution of the stock solution. Solutions (0.1 and 1 mM) of the tetrabutylammonium salts of the respective anions were prepared in THF. The concentration of sensor compounds was kept constant throughout the titration process, while adding increasing amounts of anion to the sensor solution. Then the UV-vis and fluorescence emission spectra were recorded at room temperature. The selectivity properties were explored towards  $\text{Cl}^-$ ,  $\text{Br}^-$ ,  $\text{I}^-$ ,  $\text{NO}_3^-$ ,  $\text{ClO}_4^-$ ,  $\text{BF}_4^-$ ,  $\text{PF}_6^-$ ,  $\text{AcO}^-$  and  $\text{H}_2\text{PO}_4^-$  (50  $\mu\text{M}$ ) by the sensor concentration in THF in the fluorescence spectra.

**Stoichiometry and Job's plot experiment.** Stoichiometry was determined by Job's plot method and monitored by fluorescence spectrometry. Stock solutions of the same concentration (0.2 mM) of **BNCz** and  $\text{F}^-$  anions were prepared in THF. A series of proportions of  $\text{F}^-$  varying from 0 to 1.0 was prepared with a constant total concentration (20  $\mu\text{M}$ ). After shaking the vials for a few minutes, the fluorescence emission spectra of the solutions were obtained through fluorescence titration at room temperature. Finally, the intensity changes at an emission wavelength of 483 nm against the concentration ratio of  $\text{F}^-$  to the overall concentration were obtained, namely, the Job's plot.

**Preparation of Test Strips.** Blank test strips were prepared by cutting ordinary photographic paper (2 cm  $\times$  2 cm). The strips as obtained were further treated by immersing them into the THF solution of **BNCz** ( $1 \times 10^{-3} \text{ mol} \cdot \text{L}^{-1}$ ), and then dried in air at room temperature.

**Pater Test of  $\text{F}^-$ .** The aqueous solutions of  $\text{F}^-$  with definite concentrations were prepared by diluting its stock solution ( $1 \text{ mol} \cdot \text{L}^{-1}$ ) with tap water. Then, the TBAF aqueous solutions as obtained

( $1 \times 10^{-6} \sim 1 \times 10^{-1} \text{ mol} \cdot \text{L}^{-1}$ ) and tap water were spotted onto the test strips using a micro-syringe. After evaporation of the solvent at room temperature, the test paper was illuminated with handheld UV light (365 nm). The dark spots were identified by an independent observer, and each set of experiments was repeated three times for consistency.

**Determination of Detection Limit (DL).** The detection limit of the sensor has been determined according to the following equations or functions:

$$S_b = \sqrt{\frac{\sum_{i=1}^n (x_i - \bar{x})^2}{n-1}} \quad (1)$$

$$S = \frac{\Delta I}{\Delta c} \quad (2)$$

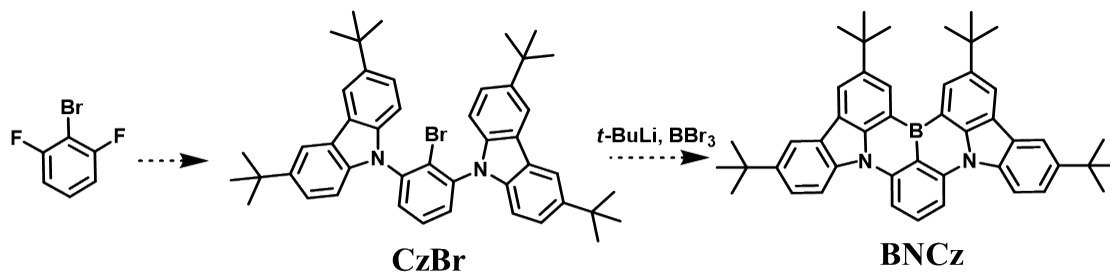
$$DL = \frac{3S_b}{S} \quad (3)$$

The standard deviation ( $S_b$ ) regarding present **BNCz** and the instrument was determined by measuring the fluorescence intensities ( $x_i$ ) of **BNCz** in THF for more than 100 times, and calculating the corresponding average intensity ( $\bar{x}$ ) firstly. By fitting the intensity data and the average intensity as obtained into equation (1), the value of the standard deviation ( $S_b$ ) was obtained.

Then,  $\text{F}^-$  was added into the solution of **BNCz** with different concentrations, and then the fluorescence emission intensities were recorded (**Figure 1b**). Corresponding variations in intensity ( $\Delta I$ ) and the  $\text{F}^-$  concentration ( $\Delta c$ ) were calculated. By fitting the data into equation(2),  $S$  value for the present system was obtained.

Finally, with the values of  $S_b$  and  $S$  as determined, the  $DL$  for the present system was calculated according to equation (3).

## Supplementary Schemes and Figures



Scheme S1. Synthetic procedures of BNCz.

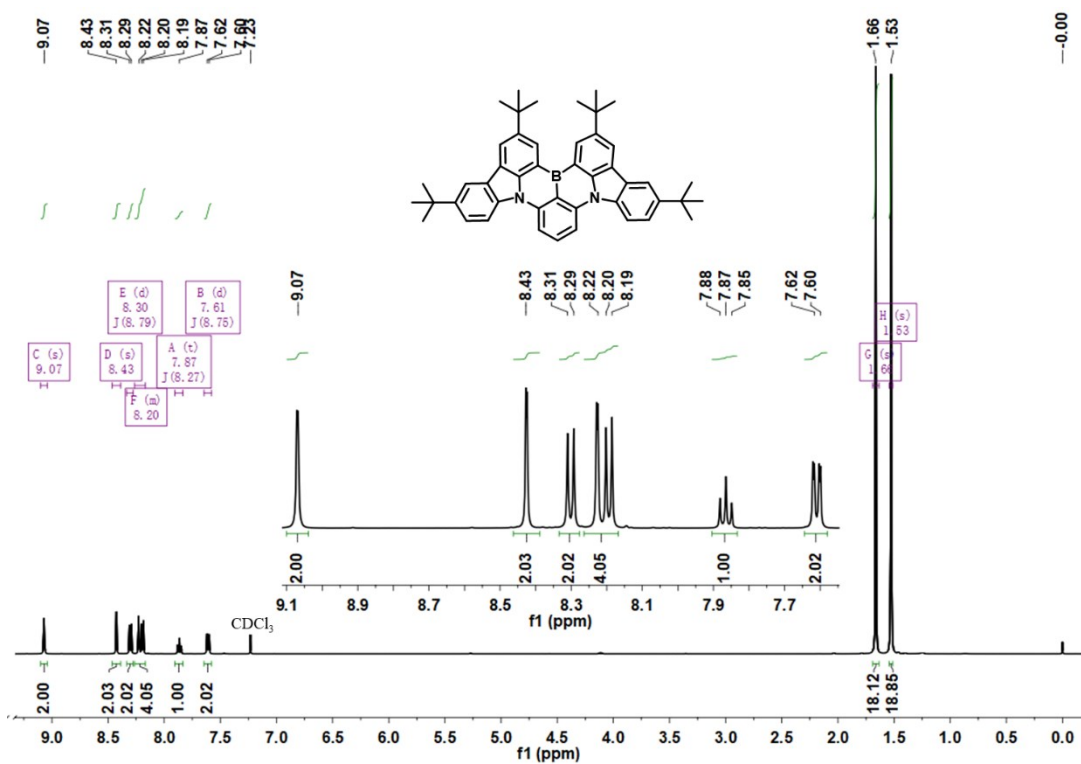


Figure S1.  $^1\text{H}$  NMR spectrum of BNCz.

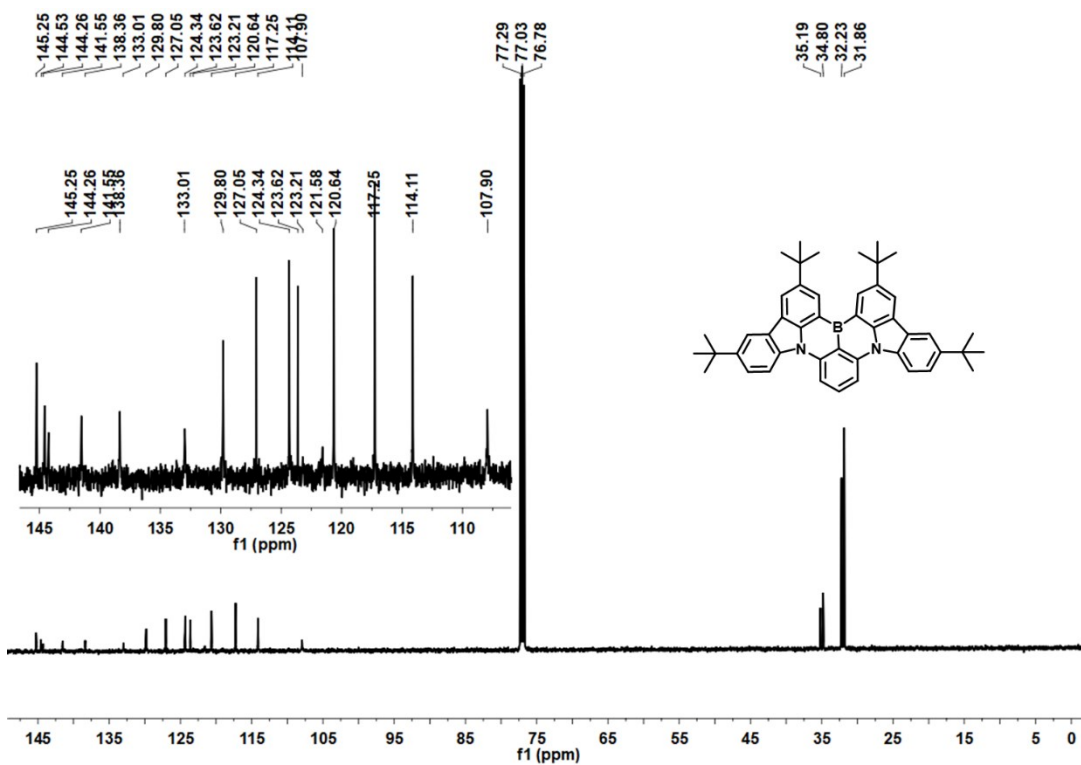


Figure S2.  $^{13}\text{C}$  NMR spectrum of BNCz.

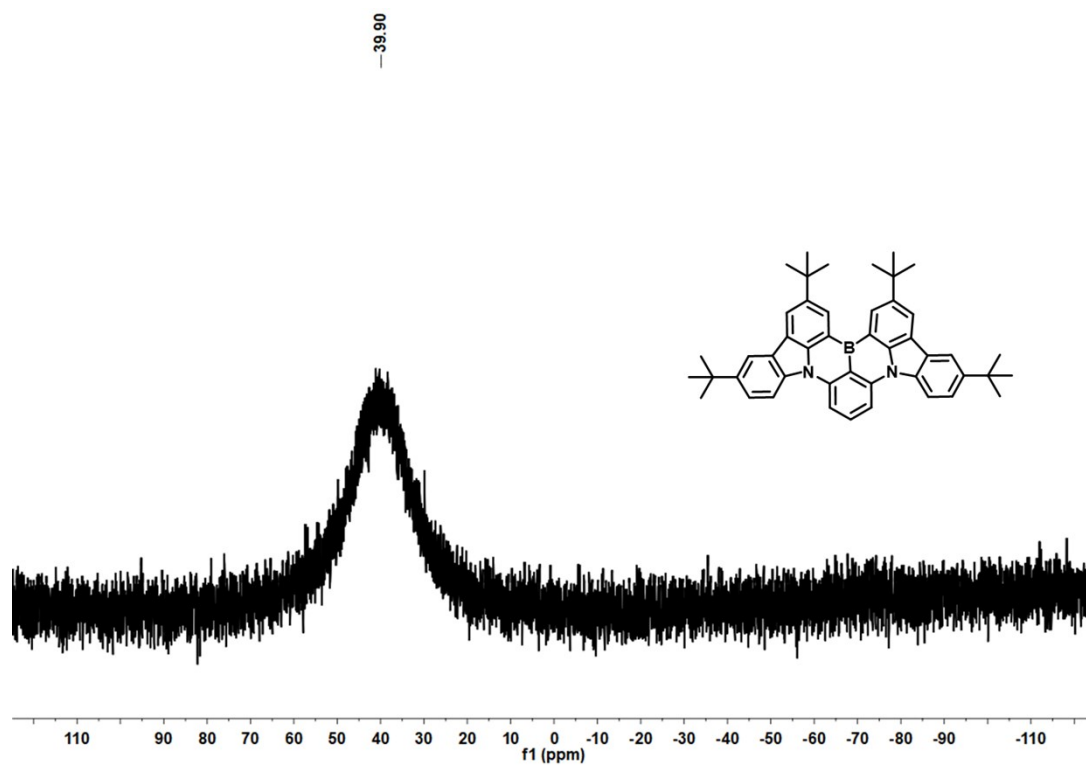


Figure S3.  $^{11}\text{B}$  NMR spectrum of BNCz.

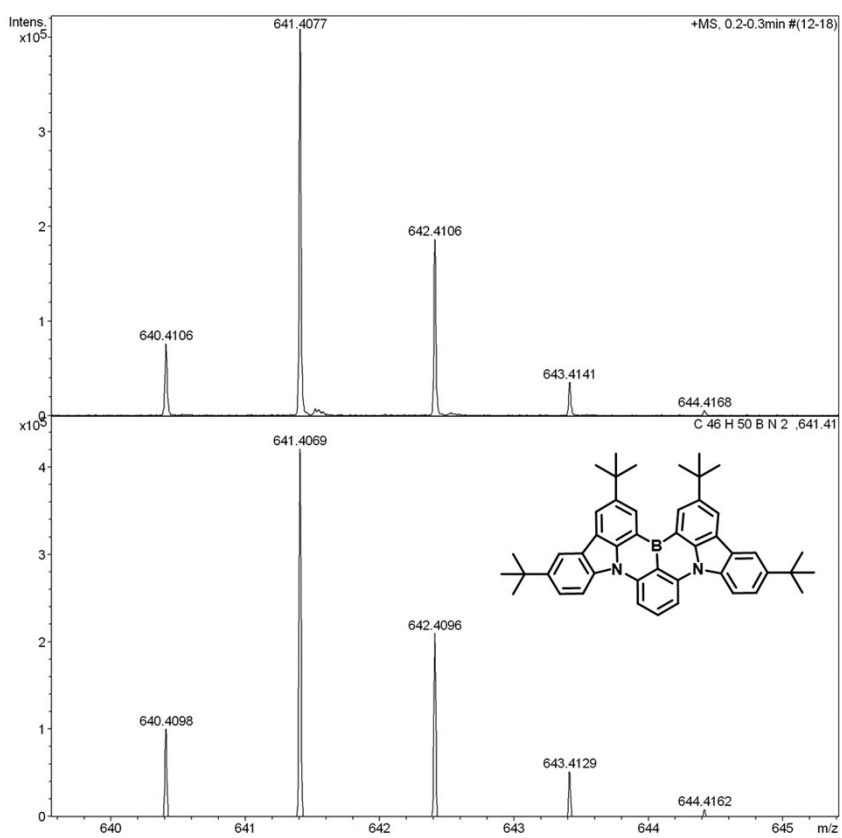
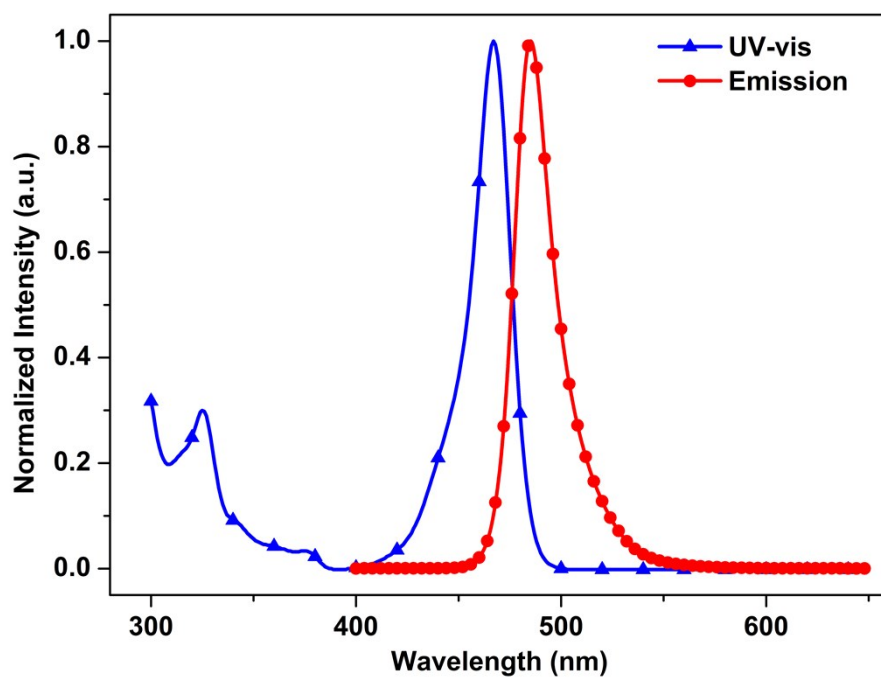
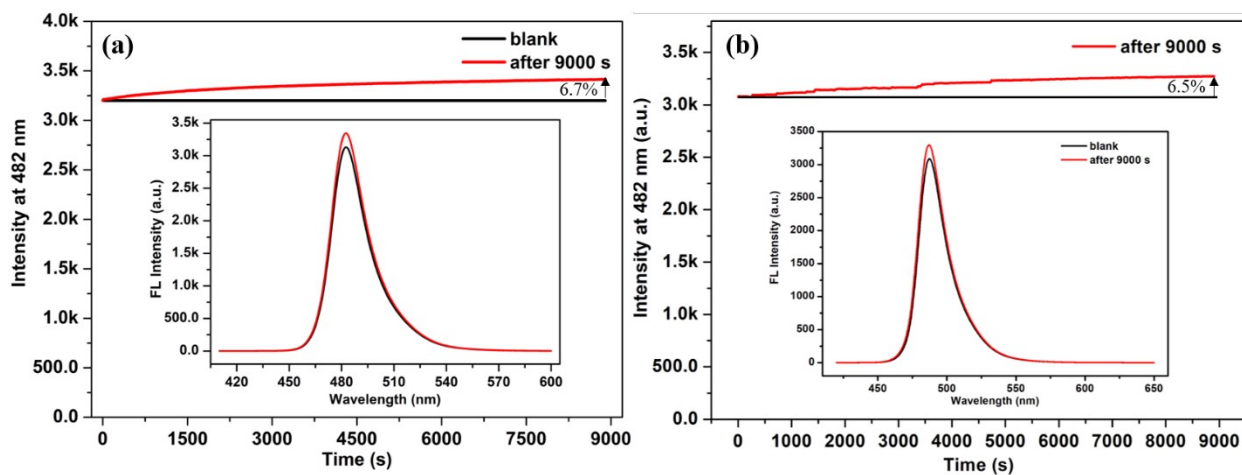


Figure S4. HRMS spectrum of BNCz.



**Figure S5.** Normalized UV–vis absorption and fluorescence emission spectra ( $\lambda_{\text{ex}}=467$  nm).





**Figure S6.** Photochemical stability monitored at 482 nm of **BNCz** in THF (a) and THF/H<sub>2</sub>O (v:v, 1:1) (b) (1  $\mu$ M). Inset is the spectra recorded before and after 2.5 h continuous irradiation.

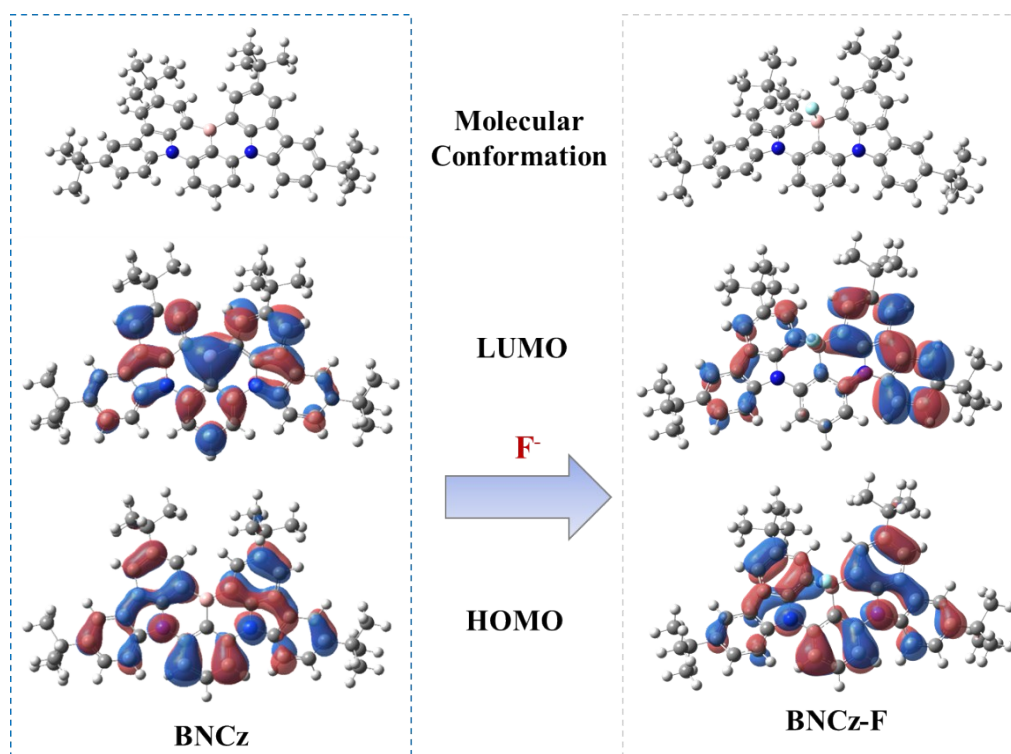


**Figure S7.** Molecular conformation and distributions of frontier molecular orbitals of **BNCz** and **BNCz-F** based on DFT calculations with B3LYP method.

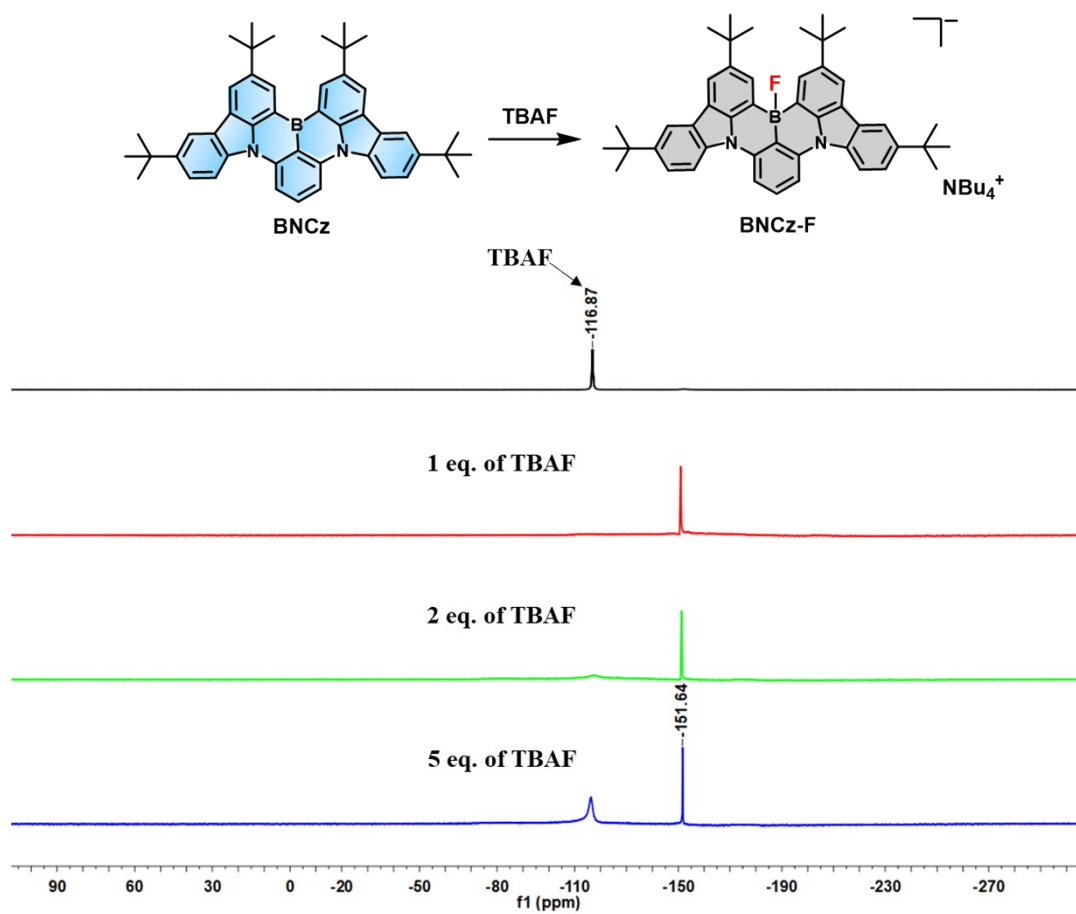


**Figure S8.** (top) Fluoride anion binding to compound **BNCz**. (bottom)  $^{19}\text{F}$  NMR spectra of a mixture of **BNCz** after addition of 1, 2 and 5 equivs. of TBAF.

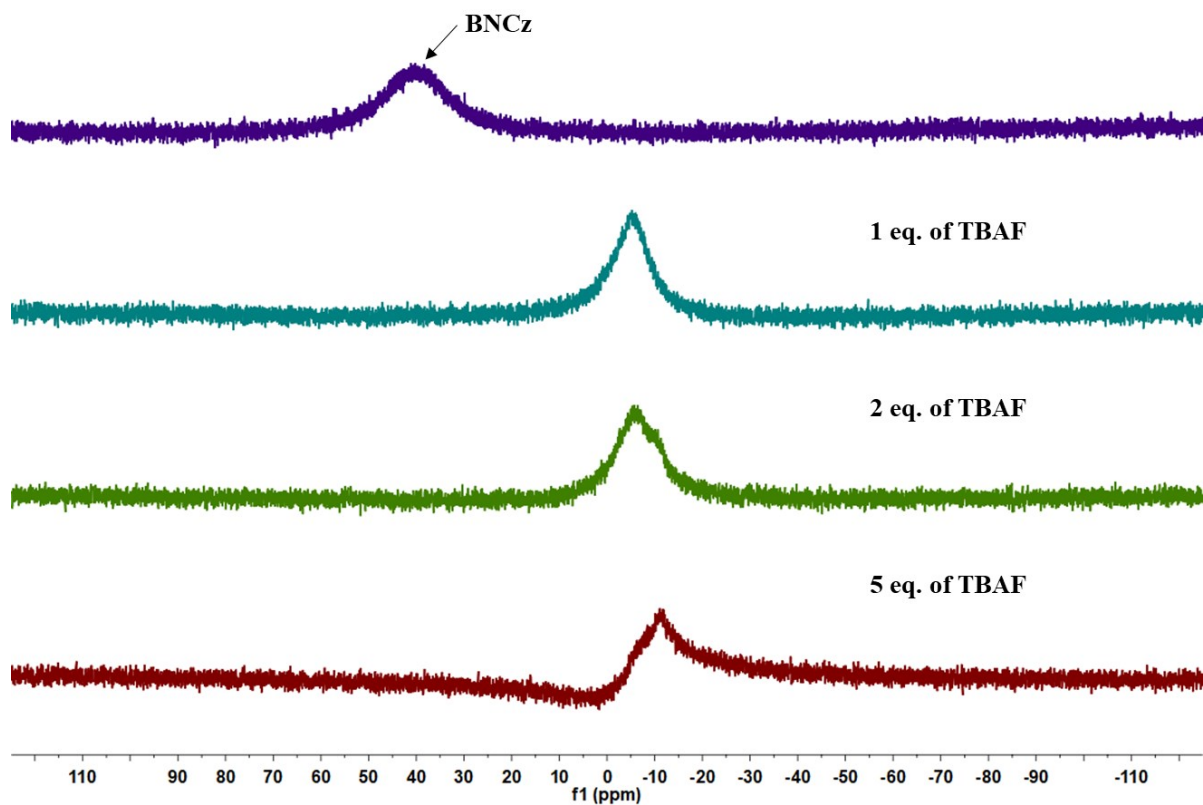


**Figure S9.**  $^{11}\text{B}$  NMR spectra of a mixture of **BNCz** after addition of 1, 2 and 5 equivs. of TBAF.

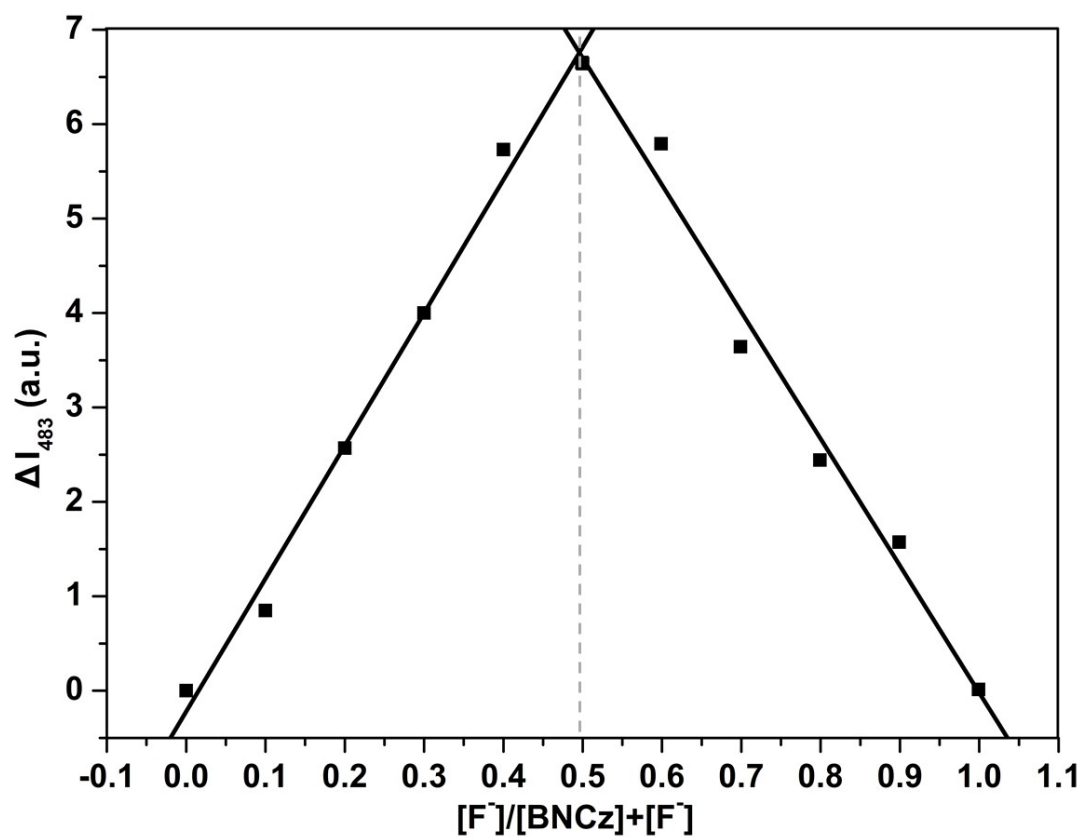


**Figure S10.** Job's Plot for complexation of **BNCz** with  $F^-$ , the total concentration for the experiments is  $20 \mu\text{M}$  ( $\lambda_{\text{ex}} = 467 \text{ nm}$ ).

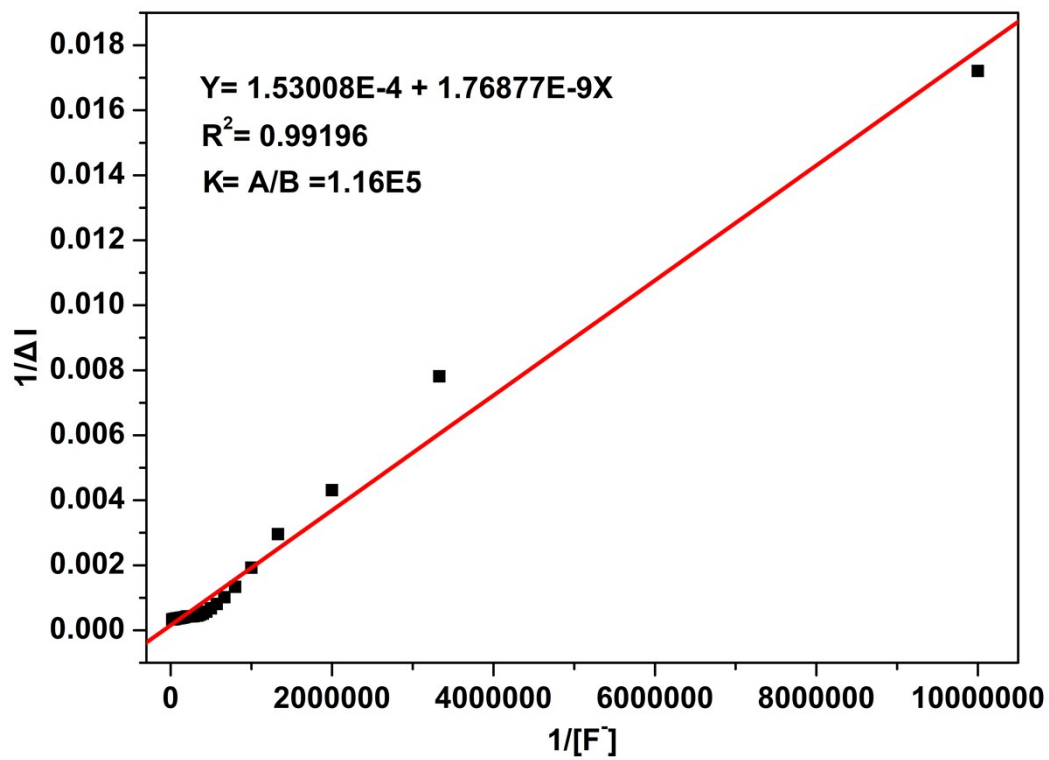
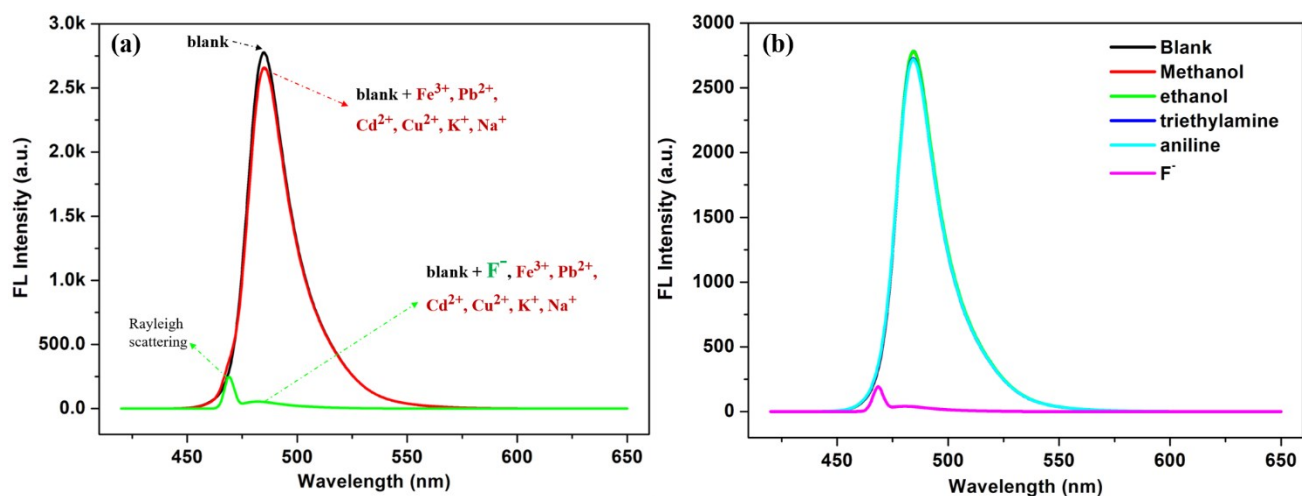
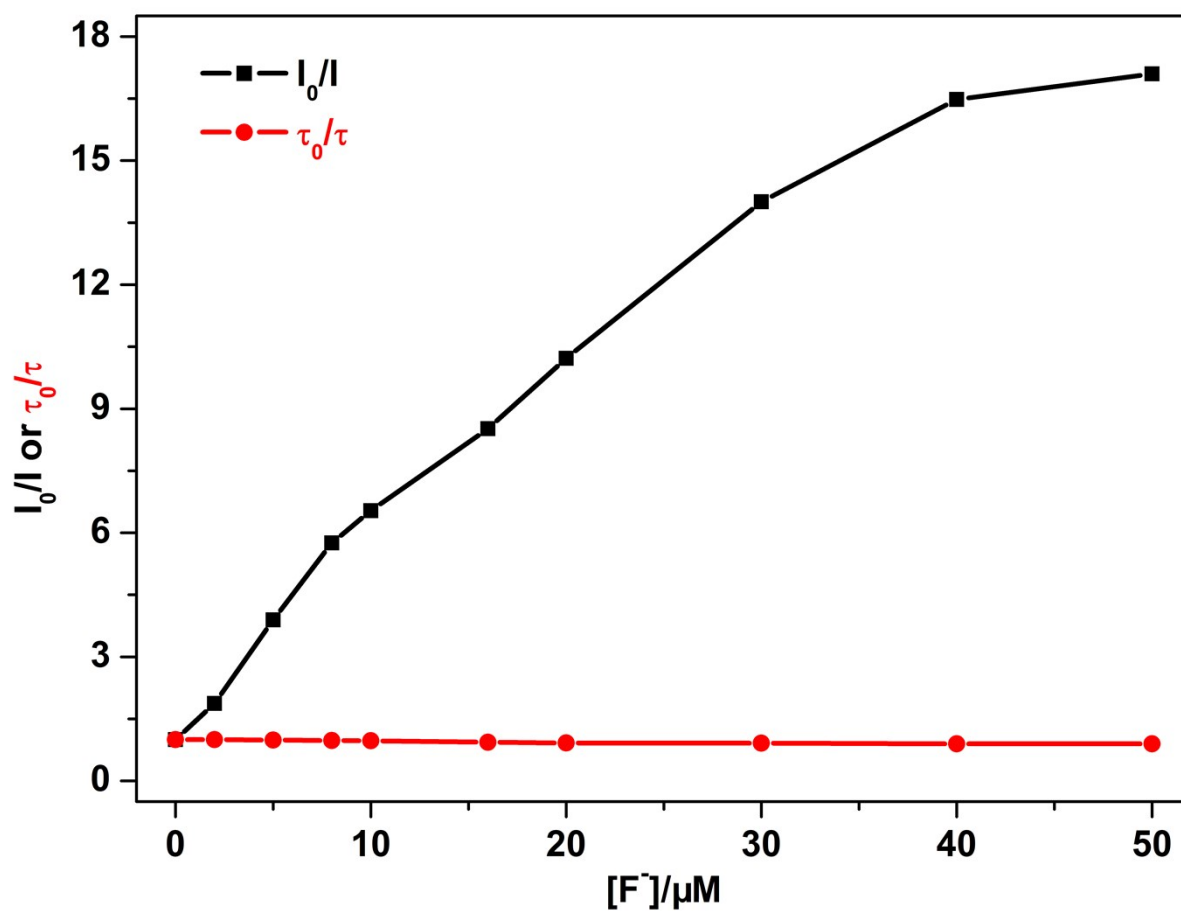


Figure S11. Benesi–Hildebrand plot for complexation of **BNCz** with  $F^-$ .



**Figure S12.** Quantitative histograms of the fluorescence responses of **BNCz** to the presence of different cations (a), alcohols and amines (b).



**Figure S13.** Stern–Volmer plots of fluorescence intensity ( $I_0/I$ ) and lifetime change ( $\tau_0/\tau$ ) as a function of  $[F^-]$  of BNCz ( $\lambda_{\text{em}} = 483 \text{ nm}$ ) in THF upon addition of  $n\text{-Bu}_4\text{NF}$ .



**Table S1.** Crystallographic data for **BNCz**.

<b>Data</b>	<b>BNCz</b>
CCDC	2032277
formula	C <sub>46</sub> H <sub>49</sub> BN <sub>2</sub>
fw	640.68
<i>T</i> /K	190.15
Wavelength/ Å	1.34139
Crystal system	monoclinic
Space group	P2 <sub>1</sub> /c
<i>a</i> /Å	27.2771(7)
<i>b</i> /Å	5.7088(2)
<i>c</i> /Å	22.7716(6)
$\alpha$ , deg	90
$\beta$ , deg	96.6240(10)
$\gamma$ , deg	90
<i>V</i> /Å <sup>3</sup>	3522.31(18)
<i>Z</i> , <i>D<sub>c</sub></i> /(g cm <sup>-3</sup> )	4, 1.208
$\mu$ /mm <sup>-1</sup>	0.333
F(000)	1376.0
2 $\theta$ /deg	5.676 to 107.992
reflns measured	28145
reflns used ( <i>R</i> <sub>int</sub> )	6423 (0.0428)
GOF on F <sup>2</sup>	1.038
Final <i>R</i> [ <i>I</i> > 2 $\sigma$ ( <i>I</i> )]	<i>R</i> <sub>1</sub> = 0.0376 w <i>R</i> <sub>2</sub> = 0.0898
<i>R</i> (all data)	<i>R</i> <sub>1</sub> = 0.0486 w <i>R</i> <sub>2</sub> = 0.0960

**Table S2.** Crystallographic data for **BNCz-FO**.

<b>Data</b>	<b>BNCz-FO</b>
CCDC	2032276
formula	$C_{61}B_{0.62}F_{0.62}N_3H_{84.15}O$
fw	893.81
<i>T</i> /K	296(2)
Wavelength/ Å	0.71073
Crystal system	monoclinic
Space group	$P2_1/c$
<i>a</i> /Å	11.5553(16)
<i>b</i> /Å	32.283(5)
<i>c</i> /Å	19.119(3)
$\alpha$ , deg	90
$\beta$ , deg	102.959(4)
$\gamma$ , deg	90
<i>V</i> /Å <sup>3</sup>	6950.5(17)
<i>Z</i> , <i>D<sub>c</sub></i> /(g cm <sup>-3</sup> )	4, 0.854
$\mu$ /mm <sup>-1</sup>	0.051
F(000)	1951.0
2 $\theta$ /deg	3.988 to 50.29
reflns measured	50537
reflns used ( <i>R</i> <sub>int</sub> )	12292 (0.0848)
GOF on F <sup>2</sup>	1.064
Final <i>R</i> [ <i>I</i> > 2 $\sigma$ ( <i>I</i> )]	$R_1 = 0.1572$ $wR_2 = 0.3471$
<i>R</i> (all data)	$R_1 = 0.2304$ $wR_2 = 0.3820$

## Coordinates of molecular structures

**Table S3.** Cartesian coordinates of optimized geometry of **BNCz** (DFT, B3LYP/6-31g\*)

Standard orientation: (Ground State)

Center Number	Atomic Number	Atomic Type	Coordinates (Angstroms)		
			X	Y	Z
1	6	0	1.239403	-1.974008	-0.014236
2	6	0	1.233726	-3.373952	0.040345
3	6	0	0.021951	-4.052244	-0.015165
4	6	0	-1.193145	-3.380414	-0.067545
5	6	0	-1.205355	-1.980398	-0.007692
6	6	0	0.014908	-1.233834	-0.010304
7	7	0	2.446307	-1.255079	-0.047560
8	7	0	-2.415410	-1.267463	0.029918
9	6	0	3.787979	-1.701626	-0.166229
10	6	0	-3.754588	-1.720654	0.157277
11	6	0	2.484650	0.121963	0.173163
12	6	0	-2.460335	0.109612	-0.186365
13	6	0	4.652735	-0.603572	0.072453
14	6	0	6.040363	-0.759048	0.017002
15	6	0	6.605211	-1.996910	-0.300537
16	6	0	5.722476	-3.058402	-0.587918
17	6	0	4.335726	-2.934343	-0.534165
18	6	0	1.378235	0.978198	0.239686
19	6	0	1.686410	2.325558	0.514893
20	6	0	2.996419	2.811153	0.683213
21	6	0	4.064766	1.906845	0.551917
22	6	0	3.815932	0.560068	0.291430
23	6	0	-4.292713	-2.957254	0.525752
24	6	0	-5.678478	-3.088938	0.589544
25	6	0	-6.569017	-2.031614	0.312231
26	6	0	-6.012933	-0.789772	-0.006311
27	6	0	-4.626918	-0.627137	-0.072085
28	6	0	-3.797558	0.542201	-0.294262
29	6	0	-4.049530	1.885227	-0.547576
30	6	0	-2.983487	2.798751	-0.686374
31	6	0	-1.674125	2.321728	-0.529613
32	6	0	-1.360852	0.970110	-0.257243
33	6	0	-3.298784	4.276149	-0.996450
34	6	0	-8.088146	-2.272423	0.387905
35	6	0	3.218696	4.305205	0.997076

36	6	0	8.126123	-2.229686	-0.365001
37	6	0	8.925597	-0.955726	-0.032815
38	6	0	8.522959	-2.687746	-1.788604
39	6	0	8.522079	-3.325400	0.653094
40	6	0	4.710881	4.656699	1.150410
41	6	0	2.504430	4.666114	2.321249
42	6	0	2.640933	5.169683	-0.148543
43	6	0	-2.027823	5.137804	-1.119500
44	6	0	-4.170387	4.868623	0.136252
45	6	0	-4.067986	4.368923	-2.335882
46	6	0	-8.896651	-1.000944	0.068514
47	6	0	-8.471095	-2.739194	1.812466
48	6	0	-8.486722	-3.365284	-0.632233
49	5	0	0.010108	0.311048	-0.010067
50	1	0	2.148555	-3.933142	0.152011
51	1	0	0.025012	-5.138466	-0.017683
52	1	0	-2.105286	-3.943518	-0.181779
53	1	0	6.668516	0.102427	0.212370
54	1	0	6.126966	-4.023798	-0.876118
55	1	0	3.725391	-3.778546	-0.820502
56	1	0	0.861290	3.021620	0.618051
57	1	0	5.088919	2.246097	0.656044
58	1	0	-3.675374	-3.798821	0.804585
59	1	0	-6.075411	-4.057470	0.877680
60	1	0	-6.647242	0.068891	-0.194193
61	1	0	-5.075811	2.227678	-0.643145
62	1	0	-0.850010	3.014399	-0.638394
63	1	0	8.709935	-0.591613	0.976985
64	1	0	9.997977	-1.169334	-0.084706
65	1	0	8.716085	-0.147324	-0.740994
66	1	0	8.020730	-3.616874	-2.072806
67	1	0	9.603184	-2.863381	-1.845764
68	1	0	8.262291	-1.926839	-2.531354
69	1	0	8.265477	-3.022798	1.673530
70	1	0	9.601448	-3.511564	0.614418
71	1	0	8.013989	-4.272591	0.449372
72	1	0	5.274353	4.455848	0.233196
73	1	0	5.179013	4.100948	1.969545
74	1	0	4.816732	5.723177	1.373594
75	1	0	2.902001	4.076039	3.153396
76	1	0	1.427854	4.480356	2.267287
77	1	0	2.648081	5.726818	2.556892
78	1	0	3.133515	4.939632	-1.098941
79	1	0	1.567634	5.005850	-0.281873

80	1	0	2.790588	6.234599	0.063191
81	1	0	-1.375058	4.789554	-1.926491
82	1	0	-1.449245	5.147538	-0.189790
83	1	0	-2.305953	6.172631	-1.343589
84	1	0	-3.645664	4.825567	1.096204
85	1	0	-4.410212	5.917156	-0.073903
86	1	0	-5.115675	4.329377	0.249393
87	1	0	-3.470331	3.962881	-3.158415
88	1	0	-4.304574	5.413076	-2.570218
89	1	0	-5.010753	3.814647	-2.304953
90	1	0	-8.685089	-0.194909	0.778777
91	1	0	-8.691623	-0.631040	-0.941416
92	1	0	-9.967450	-1.220142	0.128520
93	1	0	-8.207584	-1.980815	2.556797
94	1	0	-9.550044	-2.919719	1.877664
95	1	0	-7.962764	-3.667587	2.088075
96	1	0	-8.240644	-3.056262	-1.653332
97	1	0	-9.564654	-3.557650	-0.585200
98	1	0	-7.971662	-4.310615	-0.437552

---

Zero-point correction=	0.837624
Thermal correction to Energy=	0.881881
Thermal correction to Enthalpy=	0.882826
Thermal correction to Gibbs Free Energy=	0.761667
Sum of electronic and zero-point Energies=	-1916.147241
Sum of electronic and thermal Energies=	-1916.102984
Sum of electronic and thermal Enthalpies=	-1916.102039
Sum of electronic and thermal Free Energies=	-1916.223197

**Table S4.** Cartesian coordinates of optimized geometry of **BNCz-F** (DFT, B3LYP/6-31g\*)

Standard orientation: (Ground State)

Center Number	Atomic Number	Atomic Type	Coordinates (Angstroms)		
			X	Y	Z
1	6	0	1.312973	-1.939683	-0.505522
2	6	0	1.370262	-3.335278	-0.372567
3	6	0	0.184011	-4.061129	-0.390586
4	6	0	-1.048228	-3.418320	-0.427415
5	6	0	-1.093051	-2.013111	-0.438331
6	6	0	0.082945	-1.245671	-0.584665
7	7	0	2.502470	-1.156149	-0.462604
8	7	0	-2.334474	-1.326650	-0.317845
9	6	0	3.839558	-1.560332	-0.391084
10	6	0	-3.605969	-1.802036	0.028339
11	6	0	2.452592	0.192801	-0.065174
12	6	0	-2.441152	0.064973	-0.514189
13	6	0	4.624065	-0.489115	0.127074
14	6	0	6.006527	-0.632840	0.281424
15	6	0	6.649635	-1.818685	-0.087282
16	6	0	5.856316	-2.847379	-0.639795
17	6	0	4.477397	-2.737246	-0.802614
18	6	0	1.316956	1.008121	-0.114863
19	6	0	1.510976	2.286396	0.410548
20	6	0	2.755282	2.768482	0.898918
21	6	0	3.870326	1.928131	0.841629
22	6	0	3.722638	0.621691	0.352364
23	6	0	-4.064802	-3.054385	0.465241
24	6	0	-5.416814	-3.217121	0.757354
25	6	0	-6.362770	-2.176614	0.647164
26	6	0	-5.889048	-0.921374	0.256478
27	6	0	-4.536382	-0.723829	-0.035425
28	6	0	-3.786821	0.462384	-0.380380
29	6	0	-4.124357	1.806469	-0.557976
30	6	0	-3.123483	2.739033	-0.860122
31	6	0	-1.789552	2.282235	-0.960216
32	6	0	-1.395083	0.947859	-0.779718
33	6	0	-3.512152	4.218192	-1.067619
34	6	0	-7.842453	-2.452177	0.972367
35	6	0	2.837446	4.206571	1.449929
36	6	0	8.168361	-2.028227	0.063424
37	6	0	8.869802	-0.806179	0.685645

38	6	0	8.801221	-2.284515	-1.325112
39	6	0	8.438302	-3.247755	0.976522
40	6	0	4.250238	4.569577	1.945723
41	6	0	1.863454	4.360840	2.642291
42	6	0	2.449393	5.216665	0.343973
43	6	0	-2.299227	5.111920	-1.388807
44	6	0	-4.178507	4.767774	0.216295
45	6	0	-4.510008	4.333284	-2.244673
46	6	0	-8.721861	-1.199354	0.799639
47	6	0	-7.977743	-2.931569	2.437335
48	6	0	-8.386496	-3.550084	0.027508
49	5	0	0.089851	0.350056	-0.952281
50	1	0	2.309180	-3.850413	-0.229800
51	1	0	0.218445	-5.147068	-0.348837
52	1	0	-1.949337	-4.008975	-0.486371
53	1	0	6.571256	0.202681	0.681140
54	1	0	6.329921	-3.768279	-0.969682
55	1	0	3.931664	-3.540352	-1.280578
56	1	0	0.658151	2.960656	0.424743
57	1	0	4.845979	2.266167	1.174346
58	1	0	-3.396699	-3.887608	0.624417
59	1	0	-5.740221	-4.198764	1.093286
60	1	0	-6.559711	-0.071748	0.185540
61	1	0	-5.161356	2.117730	-0.457126
62	1	0	-1.009854	2.995324	-1.204171
63	1	0	8.481157	-0.581967	1.684287
64	1	0	9.943573	-1.002585	0.782166
65	1	0	8.750172	0.088660	0.066402
66	1	0	8.374320	-3.168924	-1.806851
67	1	0	9.883711	-2.441289	-1.236256
68	1	0	8.632742	-1.431507	-1.990505
69	1	0	8.014490	-3.087515	1.973371
70	1	0	9.516509	-3.419515	1.086849
71	1	0	7.993834	-4.161565	0.571438
72	1	0	4.988806	4.517818	1.138835
73	1	0	4.579873	3.903978	2.750505
74	1	0	4.256779	5.593765	2.336307
75	1	0	2.127745	3.669541	3.449618
76	1	0	0.831887	4.147231	2.349971
77	1	0	1.896740	5.382649	3.041946
78	1	0	3.133975	5.140759	-0.507430
79	1	0	1.437980	5.036171	-0.030328
80	1	0	2.489301	6.245216	0.725316
81	1	0	-1.794796	4.796125	-2.307051

82	1	0	-1.562857	5.101519	-0.579017
83	1	0	-2.628060	6.148608	-1.526833
84	1	0	-3.490956	4.704972	1.066240
85	1	0	-4.466502	5.819000	0.086422
86	1	0	-5.079255	4.204545	0.478067
87	1	0	-4.057962	3.965154	-3.171505
88	1	0	-4.809245	5.377775	-2.401097
89	1	0	-5.416670	3.748055	-2.063998
90	1	0	-8.409526	-0.390112	1.467619
91	1	0	-8.690642	-0.821829	-0.227567
92	1	0	-9.764708	-1.440519	1.034587
93	1	0	-7.612180	-2.167141	3.130807
94	1	0	-9.026607	-3.141821	2.681494
95	1	0	-7.403281	-3.844747	2.619228
96	1	0	-8.311594	-3.233426	-1.017973
97	1	0	-9.440425	-3.763619	0.245900
98	1	0	-7.827287	-4.484609	0.130702
99	9	0	0.462003	0.461642	-2.352477

---

Zero-point correction=	0.837948
Thermal correction to Energy=	0.883398
Thermal correction to Enthalpy=	0.884343
Thermal correction to Gibbs Free Energy=	0.761509
Sum of electronic and zero-point Energies=	-2016.073666
Sum of electronic and thermal Energies=	-2016.028216
Sum of electronic and thermal Enthalpies=	-2016.027272
Sum of electronic and thermal Free Energies=	-2016.150106



## References

1. Y. Xu, Z. Cheng, Z. Li, B. Liang, J. Wang, J. Wei, Z. Zhang and Y. Wang, *Adv. Optical Mater.*, 2020, 1902142.
2. B. Wrackmeyer, *Prog Nucl Magn Reson Spectrosc.*, 1979, **12**, 227-259.
3. K. N. Jarzemska, R. Kamiński, K. Durka, M. Kubsik, K. Nawara, E. Witkowska, M. Wiloch, S. Luliński, J. Waluk, I. Głowacki and K. Woźniak, *Dyes Pigm.*, 2017, **138**, 267-277.
4. D. L. Crossley, J. Cid, L. D. Curless, M. L. Turner and M. J. Ingleson, *Organometallics*, 2015, **34**, 5767-5774.
5. G. Sheldrick, *Acta Crystallogr. A*, 2008, **64**, 112-122.
6. Gaussian 09, Revision D.01, M. J. Frisch, G.W. Trucks, H. B. Schlegel, G. E. Scuseria, M. A. Robb, J. R. Cheeseman, G. Scalmani, V. Barone, B. Mennucci, G. A. Petersson, H. Nakatsuji, M. Caricato, X. Li, H. P. Hratchian, A. F. Izmaylov, J. Bloino, G. Zheng, J. L. Sonnenberg, M. Hada, M. Ehara, K. Toyota, R. Fukuda, J. Hasegawa, M. Ishida, T. Nakajima, Y. Honda, O. Kitao, H. Nakai, T. Vreven, J. A. Montgomery Jr., J. E. Peralta, F. Ogliaro, M. Bearpark, J. J. Heyd, E. Brothers, K.N. Kudin, V. N. Staroverov, T. Keith, R. Kobayashi, J. Normand, K. Raghavachari, Rendell, A. J.C. Burant, S. S. Iyengar, J. Tomasi, M. Cossi, N. Rega, J. M. Millam, M. Klene, J. E. Knox, J. B. Cross, V. Bakken, C. Adamo, J. Jaramillo, R. Gomperts, R. E. Stratmann, O. Yazyev, A. J. Austin, R. Cammi, C. Pomelli, J.W. Ochterski, R. L. Martin, K. Morokuma, V. G. Zakrzewski, G. A. Voth, P. Salvador, J. J. Dannenberg, S. Dapprich, A. D. Daniels, O. Farkas, J. B. Foresman, J. V. Ortiz, J. Cioslowski, D. J. Fox, Gaussian, Inc., Wallingford CT, 2013.